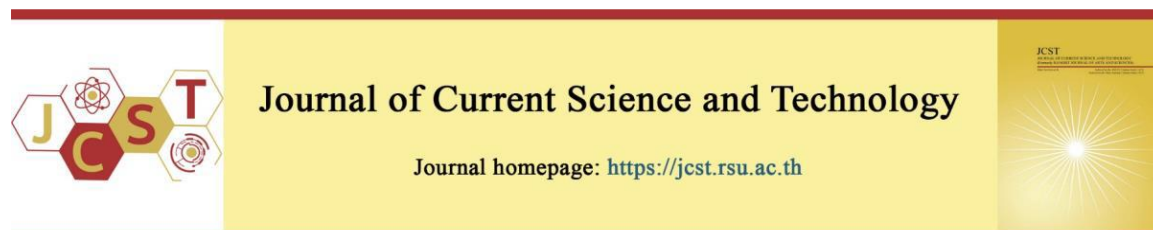


Cite this article: Bachok, Z., Saad, A. A., Zulfiqar, S., Abas, A., Shafiq, M. D., & Malik, M. F. I. A. (2024). Structural assessment of silver conductive ink using nanoindentation. *Journal of Current Science and Technology*, 14(2), Article 37. <https://doi.org/10.59796/jcst.V14N2.2024.37>



Structural Assessment of Silver Conductive Ink using Nanoindentation

Zurairhana Bachok¹, Abdullah Aziz Saad^{1*}, Sana Zulfiqar², Aizat Abas¹, Mohamad Danial Shafiq³, and Muhammad Fahirul Izwan Abdul Malik⁴

¹School of Mechanical Engineering, Universiti Sains Malaysia, 14300 Nibong Tebal, Pulau Pinang, Malaysia

²School of Mechanical and Manufacturing Engineering, National University of Science & Technology (NUST), Islamabad, 44000, Pakistan

³School of Materials and Mineral Resources Engineering, Universiti Sains Malaysia, 14300, Nibong Tebal, Pulau Pinang, Malaysia

⁴Science & Engineering Reseach Center (SERC), Universiti Sains Malaysia, 14300, Nibong Tebal, Pulau Pinang, Malaysia

*Corresponding author; E-mail: azizsaad@usm.my

Received 21 November, 2023; Revised 7 December, 2023; Accepted 6 March, 2024
Published online 2 May, 2024

Abstract

Stretchable conductive inks have emerged as a key enabling technology for the development of flexible and wearable electronic devices. Silver nanoparticles are commonly incorporated into these inks to impart electrical conductivity while maintaining stretchability. However, the amount of silver in the ink formulation can significantly influence the structural integrity and mechanical performance of printed conductive inks. This study investigates the impact of different silver contents on the structural assessment of stretchable conductive ink. Three samples of conductive inks, each with a different silver concentration (40%, 60%, and 80%) were produced by combining a PDMS-OH binder, organic solvent, cross-linking agent, catalyst, viscosity controller, additives, and silver nanoparticles. The ink samples with varying silver concentrations are characterized using nanoindentation and field-emission scanning electron microscopy (FESEM). The electrical conductivity of the silver conductive ink was measured with a digital multimeter. Among the three samples, the optimal silver concentration for conductive ink formulation is 60%, which exhibits a hardness of 2.04 MPa and an elastic modulus of 32.9 MPa to balance mechanical elasticity with an electrical conductivity of 1.389×10^4 S/m. Increasing silver content reduces the ink's flexibility, making it more brittle and less stretchable, but it also boosts its conductivity. The findings provide valuable insights into optimizing the silver content in stretchable conductive inks for achieving robust structural integrity and reliable performance in flexible and stretchable electronics.

Keywords: nanoindentation; silver conductive ink; structural assessment

1. Introduction

Conductive inks have gained significant attention in recent years for their potential in printed electronics, which offer numerous advantages such as flexibility, low-cost fabrication, and large-scale manufacturing. These electrical conductors could be used in LED displays (Kim, & Park, 2021), touch panels (Gonçalves et al., 2019; Vuorinen et al., 2014), health monitoring devices (Kim et al., 2020;

Ma, & Soin, 2022), and other electronic applications. Stretchable conductors must be able to maintain high electrical conductivity under maximum deformation (>50%) to fulfill the requirements of these new generation devices. The core component of the stretchable printed circuit is the conductive ink, which is composed of epoxy resin binder, organic solvent, cross-linking agent, catalyst, various additives, viscosity controller, and

a conductive filler. Silver (Ag) is commonly employed as a conductive material in inks owing to its excellent electrical conductivity (Ding et al., 2016; Phae-ngam et al., 2023). Moreover, silver is nowadays used in many electronic components due to the oxidative stability of silver (Krutyakov et al., 2008; Wang et al., 2016). Furthermore, in contrast to copper and aluminium, whose oxides lack conductivity, silver oxides retain their conductivity (Kamysshny, & Magdassi, 2014).

The incorporation of silver nanoparticles into these inks provides the necessary electrical conductivity while allowing the printed patterns to endure mechanical strain. However, the silver content in the ink formulation can significantly affect the structural integrity and mechanical properties of the printed conductive patterns, influencing their long-term reliability and performance which plays a crucial role in determining its printability, adhesion, and overall electrical conductivity. Various studies in the literature have reported silver contents ranging from 20 to 80 wt.% in conductive ink formulations (Ibrahim et al., 2022). However, achieving good ink stability was challenging primarily due to the high silver content in the ink, approximately 70% of silver content (Ibrahim et al., 2022).

Conductive ink material must not only possess low resistivity and high conductivity, but also adhere well to the substrate, in order to produce a stretchable printed circuit of superior quality. A notable gap in previous research lies in the insufficient attention given to stretchability control during the design phase, where the primary focus has typically been on enhancing conductivity rather than stretchability (Fernandes et al., 2020; Kim et al., 2016; Liu et al., 2019; Mo et al., 2019; Oliveira et al., 2022; Sureshkumar et al., 2015; Xu et al., 2015). Similarly, Ding revealed that the conductivity of printed electronics is dependent on the size of the silver particle distribution (Ding et al., 2016). To the best of the authors' knowledge, previous studies by Zulfiqar have explored the stretchability of silver-based conductive ink using simple uniaxial tensile testing (Zulfiqar et al., 2023) and can be referred to for future research.

Researchers employ nanoindentation testing to analyze the mechanical properties of the material under investigation to gain insight into its behavior (Bachok et al., 2022). The primary objective of this research is to develop a conductive ink that achieves both high conductivity and satisfactory

stretchability by utilizing PDMS-OH binders and silver conductive filler. However, although tensile testing was not conducted in this study to directly measure stretchability, nanoindentation was employed to gain insights into the material's brittleness and stiffness, which are key factors influencing stretchability. Materials with higher hardness, reduced modulus, and elastic modulus values tend to be stiffer and may exhibit greater susceptibility to brittle fracture. Conversely, those with lower reduced modulus and elastic modulus values may demonstrate more elastic deformation and improved stretchability. Although all three properties like hardness, reduced modulus, and elastic modulus offer some indication of a material's brittleness and stretchability, elastic modulus is particularly relevant to its ability to deform elastically under stress, thereby affecting stretchability. Additionally, the reduced modulus provides insights into both brittleness and stretchability, reflecting the material's effective stiffness near its surface.

2. Objectives

The objectives of the study are to investigate the impact of different silver contents on the assessment of stretchable conductive ink by characterizing the electrical and mechanical properties of the cured silver conductive ink in terms of hardness, reduced modulus, elastic modulus, surface morphology, and electrical conductivity.

3. Materials and methods

3.1 Conductive ink preparation

Stretchable conductive inks were prepared by combining silver powders with the base polymer of the polydimethylsiloxane (PDMS-OH) binder. A small quantity of toluene was introduced into the mixture, followed by a 24-hour stirring period on a magnetic stirrer. This process aimed to facilitate the complete dissolution of the silver powders within the PDMS-OH binder. Toluene serves as a viscosity controller. Subsequently, the mixture was added with octamethylcyclotetrasiloxane (D4), an organic solvent, and (3-Glycidyloxypropyl) trimethoxysilane (ETMS), a cross-linking agent. The resulting mixture was subjected to stirring for a duration of 3 minutes. Then, a small quantity of acetic acid and dibutyltin dilaurate (DBDTL), serving as catalysts, were added into the mixture. The finished mixture was then carefully poured into a rectangular mold that had the following measurements: 25 mm for

length, 6 mm for width, and 1 mm for thickness. The curing process was conducted under ambient conditions for a duration of 24 hours. The process of creating the conductive ink sample is illustrated in Figure 1. Various ink formulations were created by altering the proportion of silver content, i.e., 40%, 60%, and 80% (volume fraction) of silver particles, while maintaining the consistency of other components. The ink formulations were optimized in order to attain favorable levels of stretchability and electrical conductivity. The

prepared sample, as depicted in Figure 2, displays distinct characteristics on its top and bottom surfaces. The bottom surface appears notably flatter in comparison to the top surface. This difference in flatness is primarily due to shrinkage during the cooling process, resulting in excess material gathering around the edges of the top surface. As a result, the bottom surface maintains a smoother and more uniform appearance, while the top surface exhibits irregularities caused by this shrinkage-induced edge buildup.

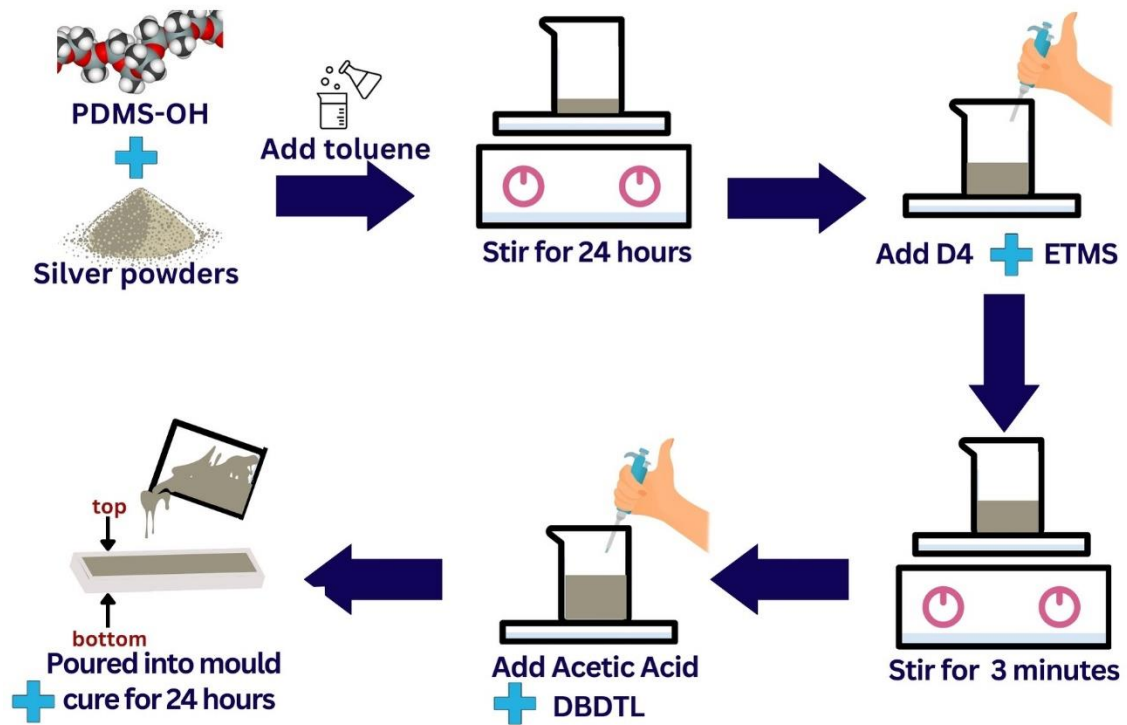


Figure 1 Conductive ink sample preparation procedure

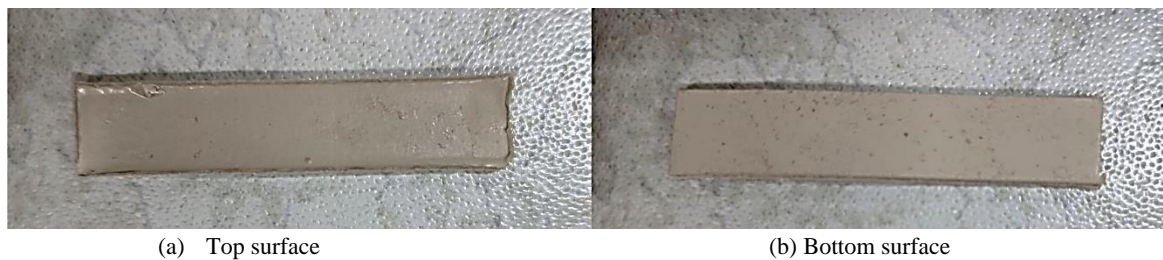


Figure 2 Example of prepared sample

3.2 Conductive ink characterization

The reliability of the developed silver conductive inks was evaluated using a nanoindenter (NanoTest Vantage, Micro Materials), a Field Emission Scanning Electron Microscope (XHR-FESEM), and a digital multimeter. This study utilizes a nanoindenter to investigate the impact of varying silver concentrations on the viscoelastic characteristics of conductive ink, specifically focusing on hardness, reduced modulus, and elastic modulus. The morphology and particle distribution of the conductive ink patterns were examined using a Field Emission Scanning Electron Microscope (FESEM), while the conductivity of the samples was measured using a digital multimeter.

The conductivity of the sample can be determined by calculating the reciprocal of its resistivity. The resistivity of each sample is tested three times in this study, and then the average value of each sample is used to calculate the resistivity and the electrical conductivity. Resistivity can be defined as the intrinsic property of a material that quantifies its resistance to the electric current flow. Resistivity is typically represented as the ratio of the resistance of conductive ink (R) to the product of length (L) and cross-sectional area of the sample (A), where A = width (W) x thickness (t). The calculation of resistivity can be expressed mathematically as:

$$\rho = \frac{RA}{L} \quad (1)$$

Then, the conductivity was calculated as:

$$\sigma = \frac{1}{\rho} \quad (2)$$

3.3 Nanoindentation testing

Hardness measurements were carried out utilizing a Nano Test Vantage nanoindenter manufactured by Micro Materials, featuring a three-sided Berkovich pyramid tip. The nanoindenter applied a 5 mN maximum load, a 1 mN/s loading rate, and a 60s dwell time. The selection of these parameters was influenced by their effects on the creep behavior and indentation dimensions at the respective maximum load levels. The determination of elastic modulus and hardness was conducted using the Oliver and Pharr equations, which have become well-known in the field of nanoindentation (Oliver, & Pharr, 2004). Figure 3 depicts a load (P)-displacement (h) curve of indentation that shows important parameters like the maximum

displacement (h_{\max}), the maximum load (P_{\max}), the loading, the unloading and the stiffness (S).

The determination of the elastic modulus and hardness values was conducted by analyzing the unloading procedures depicted in Figure 3. The study employed an angle of $\phi = 70.3^\circ$ for the Berkovich indenter, assuming that any pile-up effects were negligible. The sink-in amount (h_s), in the elastic model is determined using Equation 3. In this equation, the geometry constant of the indenter (ϵ) is assigned a specific value of = 0.75, which is specifically applicable to the indenter of Berkovich paraboloid. Equation 4 is employed to calculate the depth of contact (h_c), while Fischer-Cripps utilizes Equation 5 to determine the projected contact area. Equations 6, 7, and 8 are then used, respectively, to determine the projected area's stiffness (S), elastic modulus (E), and hardness (H). The elastic modulus (E) is calculated using a poisson ratio of silver, $\nu = 0.37$ and the geometry shape factor of the indenter, β , which is assigned a constant value of 1.034.

$$h_s = \epsilon \frac{P_{\max}}{s} \quad (3)$$

$$h_c = h_{\max} - \epsilon \frac{P_{\max}}{s} \quad (4)$$

$$A = 24.49h_c^2 \quad (5)$$

$$H = \frac{P_{\max}}{A} \quad (6)$$

$$S = \beta \frac{2}{\sqrt{\pi}} E_{\text{eff}} \sqrt{A} \quad (7)$$

$$\frac{1}{E_{\text{eff}}} = \frac{1-\nu^2}{E} + \frac{1-\nu_1^2}{E_1} \quad (8)$$

4. Results

4.1 Conductivity and surface morphology results

The resistivity and conductivity measurements of three conductive ink samples are detailed in Table 1. The results clearly indicate that higher silver content leads to increased conductivity and reduced resistivity, with sample 3, comprising 80% silver, demonstrated the highest conductivity at 4.167×10^4 S/m. The FESEM microstructure and EDX analyses of both the top and bottom surfaces of all three samples are depicted in Figures 4-6. Analysis of the material composition, based on EDX data, confirmed the presence of silver (Ag), carbon (C), silicon (Si), and tin (Sn) in the samples. Figures 5 and 6 reveal the uniform distribution of

silver particles in the 60% and 80% formulations, indicating these compositions as homogeneous polymer composites. However, EDX analyses (Figures 4(c)–6(c)) highlight a higher concentration of silver particles on the bottom surface compared to that on the top surface. Sample 1, containing 40% silver, showed no silver particles on the top surface, as shown in Figure 4 (d), indicating an uneven distribution. Similarly, the FESEM image of the bottom surface displayed an inhomogeneous distribution of silver particles due to the insufficient silver content. Figure 6 showcases the dense distribution of silver particles on the bottom surface

of the 80% formulation, and more agglomerate particles were observed on the top surface. Additionally, a notable amount of voids, highlighted by a yellow line, were observed in this sample compared to samples 1 and 2. In conclusion, among the three samples, the optimal silver concentration for the conductive ink formulation appears to be 60% of the silver content, although the 80% formulation recorded the highest conductivity. This composition exhibits a homogeneous distribution throughout the sample and the least number of voids. It also exhibits a good conductivity of 1.389×10^4 S/m.

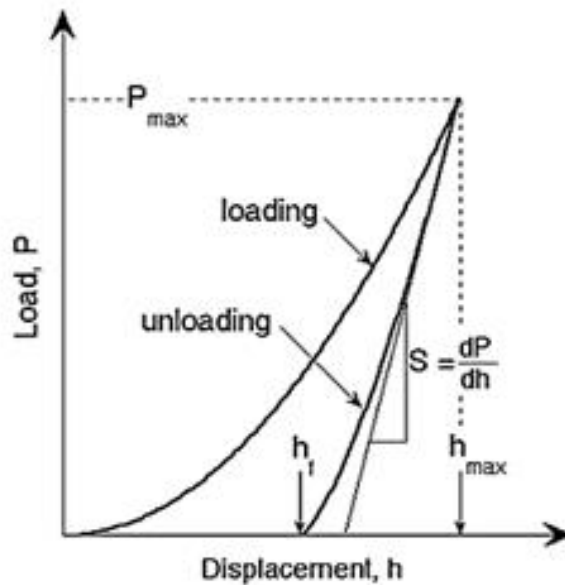


Figure 3 Load (P)-displacement (h) curve of indentation (Oliver, & Pharr, 2004)

Table 1 Resistivity and conductivity values of conductive ink samples

No	Sample	Resistivity (Ohm/m)	Conductivity (S/m)
1	Sample 1 - 40% Ag	1.4×10^{-4}	6.944×10^3
2	Sample 2 - 60% Ag	7.2×10^{-5}	1.389×10^4
3	Sample 3 - 80% Ag	2.4×10^{-5}	4.167×10^4

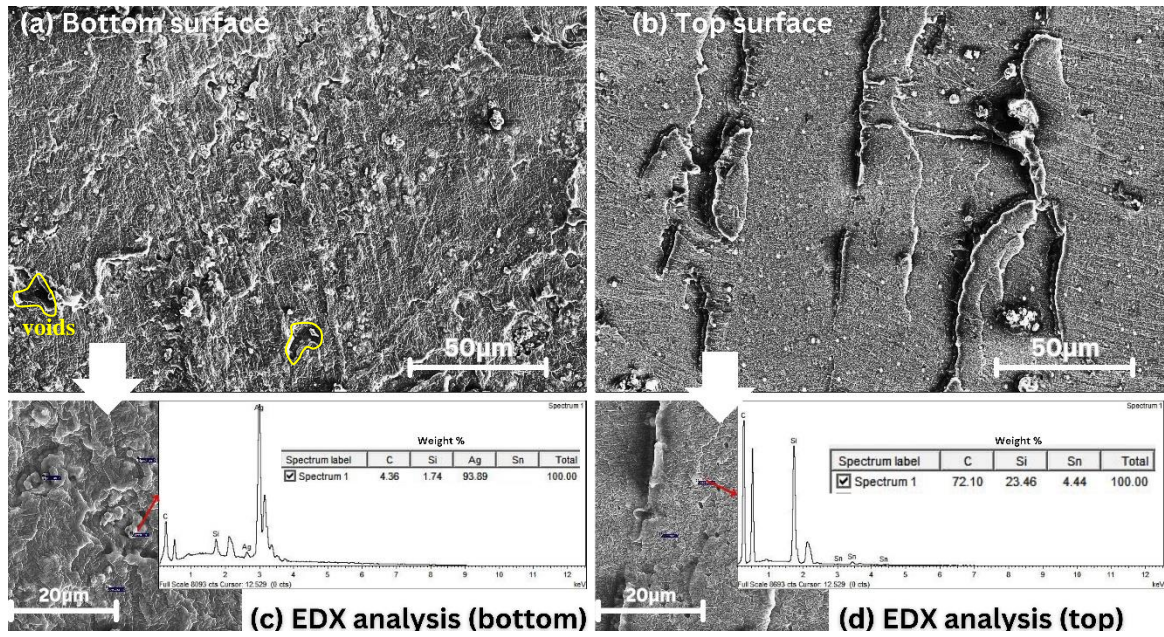


Figure 4 FESEM microstructure and EDX analysis for conductive ink with 40% silver weight (sample 1)

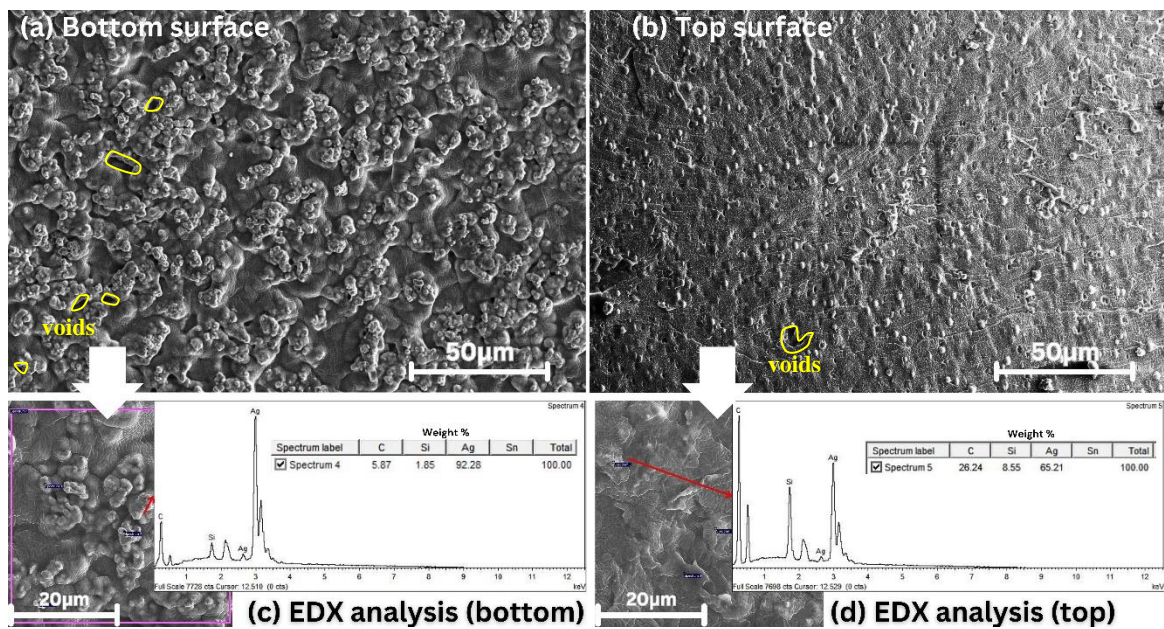


Figure 5 FESEM microstructure and EDX analysis for conductive ink with 60% silver weight (sample 2)

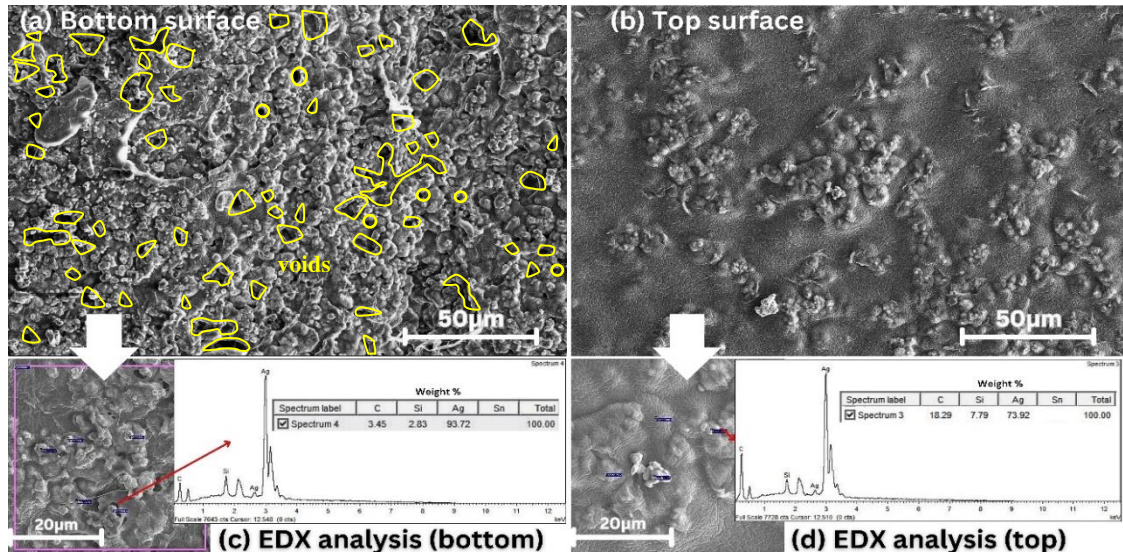


Figure 6 FESEM microstructure and EDX analysis for conductive ink with 80% silver weight (sample 3)

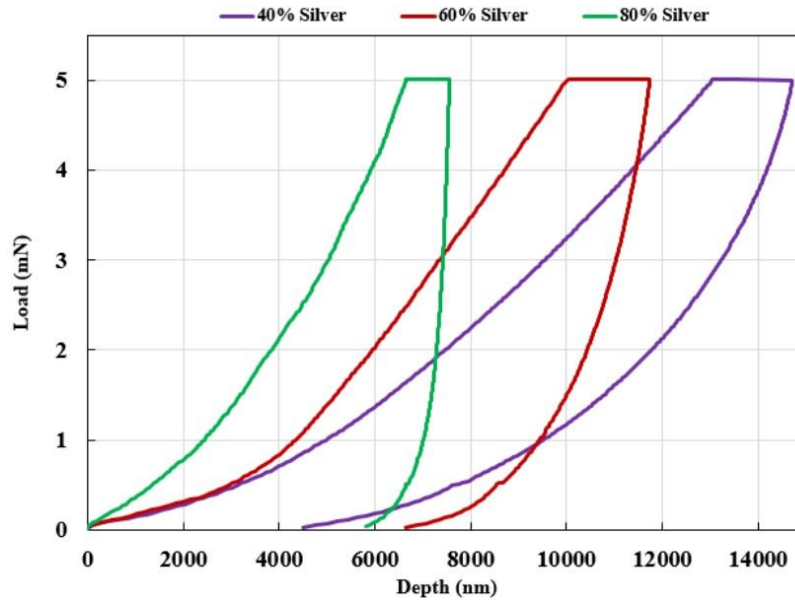


Figure 7 Load (mN) Vs depth (nm) curve of indentation for 3 conductive ink samples.

Table 2 Hardness, reduced modulus and elastic modulus of conductive ink samples

Sample	Hardness (MPa)			Reduced Modulus (MPa)			Elastic Modulus (MPa)		
	Experiment	Theoretical	% error	Experiment	Theoretical	% error	Experiment	Theoretical	% error
Sample 1 - 40% Ag	1.85	1.83	1.09	14.92	14.82	0.67	12.88	12.79	0.70
Sample 2 - 60% Ag	2.04	2.03	0.49	38.12	37.97	0.39	32.9	32.8	0.30
Sample 3 - 80% Ag	3.77	3.76	0.26	258.03	249.11	3.58	222.71	215	3.58

4.2 Hardness, reduced modulus and elastic modulus results

Figure 7 depicts the load (mN)-depth (nm) curve of indentation for the three conductive ink samples obtained using the nanoindenter machine. Meanwhile, Table 2 presents detailed results of the hardness, reduced modulus, and elastic modulus of the conductive ink samples. Furthermore, the table presents the percentage of discrepancy between the experimental and theoretical values for each outcome. Experimental results were obtained from the nanoindentation machine, while theoretical results were computed based on the Oliver-Pharr method. Hardness can be defined as the degree of resistance exhibited by a material against localized deformation. On the other hand, reduced modulus refers to the elastic behavior of a material when subjected to indentation, whereas elastic modulus represents a stiffness of a material and its ability to return to its initial shape after undergoing deformation. The load-depth curve of indentation can be described as a visual depiction that illustrates the correlation between the load applied on a system and the subsequent displacement that occurs as a result. The curve may exhibit distinct regions, including initial elastic deformation, plastic deformation, and unloading as illustrated in Figure 7. The load-displacement curve in the indentation graph reveals that, under a 5 mN load, the displacement or the depth of indentation for the 80% silver sample is shorter compared to both the 40% and 60% silver samples. The percentage of error between experimental and theoretical values is between 0.26% and 3.58% as shown in Table 2. The results indicate a direct correlation between the percentage of silver in the three samples and their corresponding hardness, reduced modulus, and elastic modulus. Increasing silver content consistently leads to elevated levels of hardness, reduced modulus, and elastic modulus across the tested samples, highlighting the influential role of silver concentration on these mechanical properties.

5. Discussion

The resistivity and conductivity values presented in Table 1 indicate that higher percentages of silver result in greater conductivity and lower resistivity. A comparison with Fernandes's work on silver conductive inks, where resistivity values ranged from 3.3 to 5.6 x 10⁻⁴ Ωm (Fernandes et al., 2020), reveals a slightly lower resistivity in our results. Notably, Fernandes used

different formulations and cured his inks at temperatures of 150°C, 200°C, and 300°C, while our formulations were cured at ambient temperature. The observed decrease in resistivity in our work can be attributed to the sintering process of silver nanoparticles, leading to necking formation, and the dissolution of organic solvents in the formulations. Despite being cured at ambient temperature, our achieved resistivity and conductivity is satisfactory. Curing temperature can significantly influence the distribution, oxidation, and overall performance of silver in the conductive ink samples. Curing at ambient temperature may offer advantages such as more uniform distribution and slower oxidation of silver, while high-temperature curing can promote faster integration of silver particles and enhance conductivity, although with a risk of increased oxidation and agglomeration. The choice of curing temperature should be carefully considered based on the desired properties and application requirements of the conductive ink samples. For instance, if the final application involves heat-sensitive substrates or components, ambient curing might be preferred (Ibrahim et al., 2022).

Based on the FESEM images presented in Figures 4–6, it is evident that there is a notable disparity in the concentration of silver particles between the bottom and top surfaces of the samples. This discrepancy can be attributed to the higher density of silver compared to silicon, tin, and carbon elements. During the curing process, which involves settling over time, the heavier silver particles tend to precipitate towards the bottom of the sample, given their greater gravitational influence. When the conductive ink mixture is poured into the rectangular mold, any sedimentation or settling tendency is influenced by the relative densities of its components. Due to its higher density, silver is more prone to migrate downward under the influence of gravity (Ibrahim et al., 2022) compared to lighter components like silicon, tin, and carbon. If the ink viscosity is low enough to allow for particle movement during curing, the heavier silver particles may gradually settle towards the bottom of the mold, leading to a concentration gradient with higher silver concentrations at the bottom and lower concentrations towards the top surface of the cured sample. Moreover, volatile solvents evaporate from the surface of the sample during the curing process. As these solvents evaporate, they can contribute to

a reduction in volume, leading to shrinkage of the material as shown on top surface of sample in Figure 2 (a).

The FESEM images of samples 2 and 3 illustrate differences in void formation. Sample 2 displays a more homogeneous microstructure with minimal voids, while sample 3 exhibits a higher number of voids with densely agglomerated particles. These voids, highlighted by yellow lines, indicate regions within the sample where material is absent, creating discontinuities or weak points in the structure. The prevalence of voids is more pronounced in the 80% formulation, suggesting that the higher concentration of silver particles may have impeded ink mixture homogeneity, leading to inadequate dispersion and void formation during curing. These voids can significantly influence the mechanical properties of the sample, rendering it more brittle and less resilient to mechanical stress. Ibrahim agreed that the agglomerated particles occurred when the dispersed silver particles aggregated due to the high van der Waals attraction (Ibrahim et al., 2022). She reported that it was difficult to achieve good ink stability due to the high silver content, even though it's more conductive (Ibrahim et al., 2022). Consequently, 60% of silver (sample 2) is considered the optimal formulation among the three, as shown in Figure 5, due to its better dispersion and minimized void formation.

Increasing the weightage of silver particles enhances conductivity but compromises stretchability, potentially causing rupture at larger deformations. Although this work does not cover tensile testing to analyze stretchability directly, nanoindentation results can still offer valuable insights into the brittleness of materials, essential for understanding their mechanical behavior and applications. Materials with high hardness and elastic modulus but low fracture toughness are typically more brittle, prone to fracturing under stress without significant plastic deformation. Conversely, those with lower hardness and elastic modulus but higher fracture toughness tends to be more ductile and resistant to brittle fracture. Additionally, the increased viscosity of the ink due to higher silver content renders the final sample more brittle (Larmagnac et al., 2014). Balancing stretchability and conductivity require optimizing the elastomer/conductive filler ratio. Augmenting the PDMS (elastomer) content enhances stretchability and flexibility but risks weakening the bond between silver particles (conductive filler) and the PDMS

matrix, leading to increased electrical resistance. The bond between silver particles and PDMS is crucial for maintaining good electrical conductivity. The findings demonstrate a clear relationship between the silver content in the three samples and their respective measures of hardness, reduced modulus, and elastic modulus. Sample 3, which contains the highest silver content, demonstrates significantly higher reduced modulus and elastic modulus values compared to samples 1 and 2. The increase in silver content resulted in a decrease in material strength and stiffness while concurrently decreasing stretchability. Careful formulation and processing techniques are necessary to ensure proper dispersion and bonding of silver particles within the PDMS matrix, achieving desirable stretchability and low electrical resistance in printed electronic circuits.

6. Conclusion

In conclusion, this study investigated the influence of silver contents and curing temperature on the conductivity, resistivity, microstructure, and mechanical properties of conductive ink samples. Increasing of the silver contents improved conductivity but compromised stretchability, potentially leading to rupture at larger deformations. Nanoindentation results provided valuable insights into the brittleness of the materials, with higher hardness and elastic modulus associated with increased brittleness. The results show that an increase in silver in the formulation led to higher hardness and elastic modulus, reducing stretchability and increasing viscosity. The presence of voids, particularly in samples with highest silver content, significantly impacted the mechanical properties, rendering them more brittle and less resilient to mechanical stress. It shows that a 60% silver concentration strikes a balance between properties, making it optimal for ink formulation. The formulation's enhanced dispersion and reduced void formation, coupled with its hardness of 2.04 MPa, elastic modulus of 32.9 MPa, and conductivity of 1.389×10^{-4} S/m, render it well-suited for utilization in thermally sensitive devices. The findings highlight the importance of balancing stretchability and conductivity by optimizing the elastomer/conductive filler ratio and carefully considering curing temperature. Curing at ambient temperature offers advantages such as more uniform distribution and slower oxidation of silver, while high-temperature curing can enhance conductivity at the expense

of increased oxidation and agglomeration. Additionally, proper formulation and processing techniques are crucial to ensure the dispersion and bonding of silver particles within the elastomer matrix, achieving desirable stretchability and low electrical resistance in printed electronic circuits. Overall, this study provides valuable insights for the development of conductive ink formulations with tailored properties for specific applications.

7. Acknowledgements

The authors would like to thank Universiti Sains Malaysia (USM) for funding this project under Short Term Grant 304.PMEKANIK.6315494.

8. References

- Bachok, Z., Saad, A., Abas, M., Ali, M., & Fakpan, K. (2022). Structural analysis on nanocomposites lead free solder using nanoindentation. *Journal of Advanced Manufacturing Technology*, 16(2), 15–28. <https://jamt.utem.edu.my/jamt/article/view/6383>
- Ding, J., Liu, J., Tian, Q., Wu, Z., Yao, W., Dai, Z., Liu, L., & Wu, W. (2016). Preparing of Highly Conductive Patterns on Flexible Substrates by Screen Printing of Silver Nanoparticles with Different Size Distribution. *Nanoscale Research Letters*, 11(1), Article 412. <https://doi.org/10.1186/s11671-016-1640-1>
- Fernandes, I. J., Aroche, A. F., Schuck, A., Lamberty, P., Peter, C. R., Hasenkamp, W., & Rocha, T. L. A. C. (2020). Silver nanoparticle conductive inks: synthesis, characterization, and fabrication of inkjet-printed flexible electrodes. *Scientific Reports*, 10(1), Article 8878. <https://doi.org/10.1038/s41598-020-65698-3>
- Gonçalves, S., Serrado-Nunes, J., Oliveira, J., Pereira, N., Hilliou, L., Costa, C. M., & Lanceros-Méndez, S. (2019). Environmentally Friendly Printable Piezoelectric Inks and Their Application in the Development of All-Printed Touch Screens. *ACS Applied Electronic Materials*, 1(8), 1678–1687. <https://doi.org/10.1021/acsaelm.9b00363>
- Ibrahim, N., Akindoyo, J. O., & Mariatti, M. (2022). Recent development in silver-based ink for flexible electronics. *Journal of Science: Advanced Materials and Devices*, 7(1), Article 100395. <https://doi.org/10.1016/j.jsamd.2021.09.002>
- Kamyshny, A., & Magdassi, S. (2014). Conductive Nanomaterials for Printed Electronics. *Small*, 10(17), 3515–3535. <https://doi.org/10.1002/sml.201303000>
- Kim, E., Lim, D. Y., Kang, Y., & Yoo, E. (2016). Fabrication of a stretchable electromagnetic interference shielding silver nanoparticle/elastomeric polymer composite. *RSC Advances*, 6(57), 52250–52254. <https://doi.org/10.1039/c6ra04765c>
- Kim, J.-H., & Park, J.-W. (2021). Intrinsically stretchable organic light-emitting diodes. *Science Advances*, 7(9), 1–11. <https://doi.org/10.1126/sciadv.abd9715>
- Kim, K., Kim, B., & Lee, C. H. (2020). Printing Flexible and Hybrid Electronics for Human Skin and Eye-Interfaced Health Monitoring Systems. *Advanced Materials*, 32(15), 1–22. <https://doi.org/10.1002/adma.201902051>
- Krutyakov, Y. A., Kudrinskiy, A. A., Olenin, A. Y., & Lisichkin, G. V. (2008). Synthesis and properties of silver nanoparticles: advances and prospects. *Russian Chemical Reviews*, 77(3), 233–257. <https://doi.org/10.1070/RC2008v077n03ABEH003751>
- Larmagnac, A., Eggenberger, S., Janossy, H., & Vörös, J. (2014). Stretchable electronics based on Ag-PDMS composites. *Scientific Reports*, 4(1), Article 7254. <https://doi.org/10.1038/srep07254>
- Liu, P., He, W. Q., & Lu, A. X. (2019). Preparation of low-temperature sintered high conductivity inks based on nanosilver self-assembled on surface of graphene. *Journal of Central South University*, 26(11), 2953–2960. <https://doi.org/10.1007/s11771-019-4227-z>
- Ma, L.-Y., & Soin, N. (2022). Recent Progress in Printed Physical Sensing Electronics for Wearable Health-Monitoring Devices: A Review. *IEEE Sensors Journal*, 22(5), 3844–3859. <https://doi.org/10.1109/JSEN.2022.3142328>
- Mo, L., Guo, Z., Wang, Z., Yang, L., Fang, Y., Xin, Z., ... & Li, L. (2019). Nano-Silver Ink of High Conductivity and Low Sintering Temperature for Paper Electronics. *Nanoscale Research Letters*, 14, 1–11. <https://doi.org/10.1186/s11671-019-3011-1>

- Oliveira, A. E. F., Pereira, A. C., de Resende, M. A. C., & Ferreira, L. F. (2022). Synthesis of a silver nanoparticle ink for fabrication of reference electrodes. *Talanta Open*, 5, Article 100085. <https://doi.org/10.1016/j.talo.2022.100085>
- Oliver, W. C., & Pharr, G. M. (2004). Measurement of hardness and elastic modulus by instrumented indentation: Advances in understanding and refinements to methodology. *Journal of Materials Research*, 19(1), 3–20. <https://doi.org/10.1557/jmr.2004.19.1.3>
- Phae-ngam, W., Kamoldilok, S., Rattana, T., Lertvanithphol, T., Mungchamnankit, A. (2023). Preparation and characterization of low-emissivity AlN/Ag/AlN films by Magnetron co-sputtering method. *Journal of Current Science and Technology*, 13(3), 533-541. <https://doi.org/10.59796/jcst.V13N3.2023.498>
- Sureshkumar, M., Na, H. Y., Ahn, K. H., & Lee, S. J. (2015). Conductive nanocomposites based on polystyrene microspheres and silver nanowires by latex blending. *ACS Applied Materials and Interfaces*, 7(1), 756–764. <https://doi.org/10.1021/am5071392>
- Vuorinen, T., Zakrzewski, M., Rajala, S., Lupo, D., Vanhala, J., Palovuori, K., & Tuukkanen, S. (2014). Printable, transparent, and flexible touch panels working in sunlight and moist environments. *Advanced Functional Materials*, 24(40), 6340–6347. <https://doi.org/10.1002/adfm.201401140>
- Wang, D. Y., Chang, Y., Wang, Y. X., Zhang, Q., & Yang, Z. G. (2016). Green water-based silver nanoplate conductive ink for flexible printed circuit. *Materials Technology*, 31(1), 32–37. <https://doi.org/10.1179/1753555715Y.000000023>
- Xu, W., Xu, Q., Huang, Q., Tan, R., Shen, W., & Song, W. (2015). Electrically conductive silver nanowires-filled methylcellulose composite transparent films with high mechanical properties. *Materials Letters*, 152, 173–176. <https://doi.org/10.1016/j.matlet.2015.03.111>
- Zulfiqar, S., Saad, A. A., Ahmad, Z., & Bachok, Z. (2023). Mechanical Analysis and Constitutive Modeling of Nonlinear Behavior of Silver-based Conductive Ink. *International Journal of Automotive and Mechanical Engineering*, 20(3), 10635–10648. <https://doi.org/10.15282/ijame.20.3.2023.07.0821>